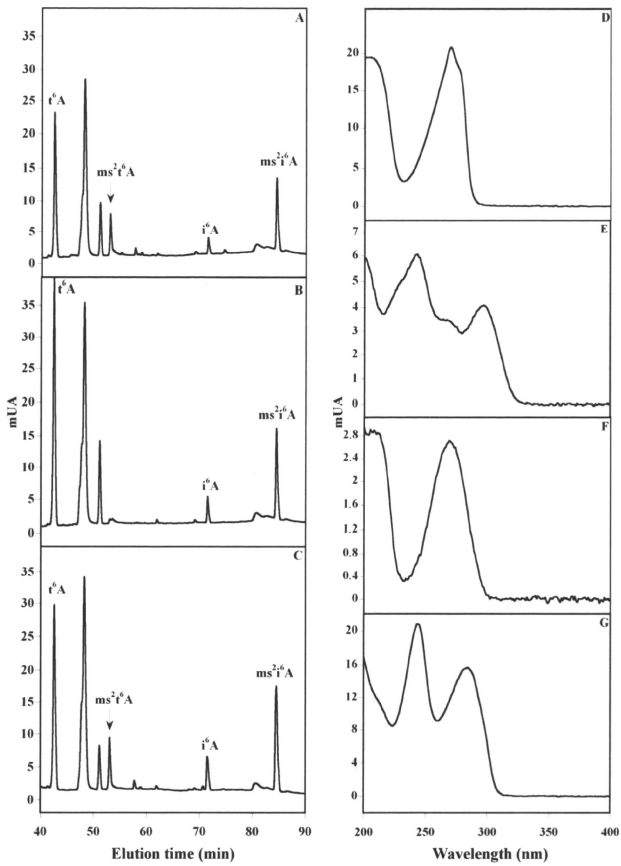

FIGURE 3. **HPLC and UV-visible detection of t^6A, ms^2t^6A, i^6A, and ms^2i^6A modified nucleosides using *B. subtilis*.** The chromatograms correspond to the analysis (45–90-min region) of bulk tRNA from the following: MGNA-001 *B. subtilis* wild-type strain (*A*); MGNA-C496 *B. subtilis yqeV*$^-$ strain (*B*); MGNA-C496 *B. subtilis yqeV*$^-$ strain complemented with the pDB148-yqeV plasmid (*C*). The UV-visible spectra of the t^6A (*D*), ms^2t^6A (*E*), i^6A (*F*), and ms^2i^6A (*G*) are shown. The experiments have been run in triplicate, and the areas have been found to be reproducible within a 5% margin error. *mAU*, milli-arbitrary units.

involved in the transformation of t^6A into ms^2t^6A, we analyzed bulk tRNA extracted from the following: (i) *B. subtilis* wild-type strain (MGNA-A001); (ii) *yqeV*-strain (MGNA-C496) lacking the *mtab* gene; and (iii), MGNA-C496 complemented with a plasmid containing the *yqeV (mtab)* gene. Bulk tRNAs were isolated after growth at 37 °C, hydrolyzed, and processed for HPLC analysis of their modified nucleosides, as described previously (24). Under these conditions, chromatograms of tRNA hydrolysates from the *B. subtilis* wild-type MGNA-A001 strain showed, as expected, in the 45–90-min region the presence of t^6A, ms^2t^6A, i^6A, and ms^2i^6A that elutes at 42, 53, 71, and 85 min, respectively (Fig. 3*A*). The identity of the four modified nucleosides was established by their chromatographic retention times and UV-visible spectra (Fig. 3, *A* and *D–G*) (24). In Fig. 3*B* is shown the HPLC of tRNA hydrolysates obtained from MGNA-C496 strain. The analysis revealed that the 53-min peak detected on the UV trace in the parental strain (MGNA-A001), corresponding to the ms^2t^6A, disappeared in the MGNA-C496 strain, and the t^6A peak increased in intensity. The ms^2t^6A peak was recovered when this strain was transformed with a plasmid carrying the wild-type *yqeV/mtaB* gene (plasmid pDB148-mtaB) confirming that the absence of ms^2t^6A modification in tRNAs extracted from the MGNA-C496 was due to the loss of *yqeV/mtaB* gene.

In Vitro Characterization of the B. subtilis MtaB (YqeV) Protein—We concentrated initially on purification and *in vitro* characterization of the *B. subtilis* YqeV/MtaB protein because of the generally greater difficulty of purifying human proteins in functional form. Induction of YqeV/MtaB expression from plasmid pT_7-*mtab* in *E. coli* strain BL21(DE3)RIL resulted in the overproduction of a protein migrating at ~50,000 Da on SDS gels, in good agreement with the molecular mass deduced from amino acid sequence (51,657 Da). The expressed protein was found in the soluble fraction of cell-free extracts. After the final step of purification, the purity was evaluated by SDS-PAGE to be over 95% (Fig. 4*A*). The as-purified protein was light brown in color and found to contain low amounts of both iron and sulfur atoms (<0.2 iron, sulfur per monomer). This suggested the presence of a protein-bound iron-sulfur cluster, however, in substoichiometric amounts, probably as a consequence of cluster losses during aerobic purification. Anaerobic treatment of the protein solution with an excess of ferrous iron and enzymatically produced sulfide generated a form of YqeV/MtaB protein, which after desalting contained up to 7.5 ± 0.2 iron and 7.5 ± 0.5 sulfur atoms per polypeptide chain, suggesting the presence of two [4Fe-4S] clusters.

The UV-visible spectrum of reconstituted MtaB (Fig. 4*B trace 2*) displays a broad absorption band centered at around

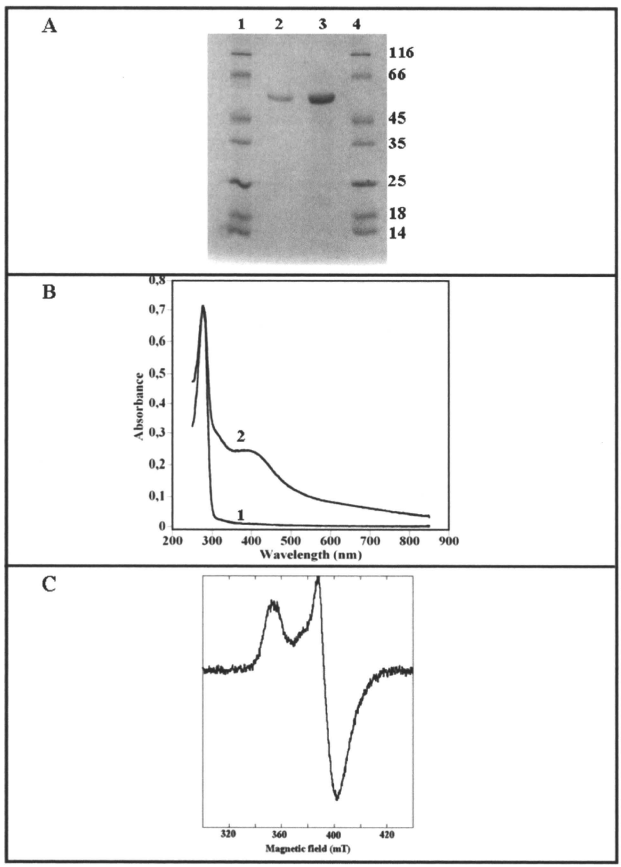

FIGURE 4. **Biochemical and spectroscopic characterization of MtaB protein.** *A*, SDS-polyacrylamide (12%) gel of MtaB after Superdex 75 chromatography (2 and 6 μg, *lanes 2* and *3*, respectively). Molecular weight markers are in *lanes 1* and *4*. *B*, light absorption spectra of apo-MtaB (4 μM) (*trace 1*) and holo-MtaB (8 μM) (*trace 2*) MtaB in 50 mM Tris-Cl, pH 8.0, with 50 mM KCl. *C*, X-band EPR spectrum of the reduced holo-MtaB (100 μM) MtaB in 50 mM Tris-Cl, pH 8.0, with 50 mM KCl. Experimental conditions are as follows: microwave power, 100 microwatts; microwave frequency, 9.6 GHz; modulation amplitude 1 millitesla; temperature 12 K.

420 nm, which is assigned to sulfur-to-iron charge transfer transitions characteristic of a $[4Fe\text{-}4S]^{2+}$ cluster. This absorption band has an A_{420}/A_{280} ratio of 0.34 ± 0.02 and a molar extinction coefficient at 400 nm of 30,000 mM^{-1} cm^{-1} in the lower range of most biological $[4Fe\text{-}4S]^{2+}$ centers (ϵ_{420} = 15–17 mM^{-1} cm^{-1} on a per cluster basis) suggesting that the reconstituted protein contains slightly less than two [4Fe-4S] clusters per polypeptide chain. Upon addition of dithionite, the absorption decreased over the entire 350–700 nm range, as expected upon reduction of the chromophore to the $[4Fe\text{-}4S]^{+}$ state (data not shown). EPR analysis of the resulting reduced protein confirmed the presence of S = ½, $[4Fe\text{-}4S]^{1+}$ centers (Fig. 4*C*).

Conclusion—The physiological role of CDKAL1/*e-MtaB* gene in eukaryotic cells remains to be elucidated. However, its similarity to *CDK5RAP1* led to the speculation that it might play an important role in insulin production under glucotoxic conditions through interaction with CDK5 that belongs to the well known large family of cyclin-dependent kinases 16). Our *in vivo* studies now indicate that it encodes a radical AdoMet MTTase that is involved in biosynthesis of 2-methylthio-N^6-threonylcarbamoyladenosine (ms^2t^6A) in tRNA. We have also shown that *B. subtilis yqeV/mtaB* encodes a protein with equivalent biochemical activity, even though it belongs to a different MTTase sequence family. Thus, ms^2t^6A is synthesized through the conversion of A to t^6A by the action of YrdC/Sua5 enzymes, as recently shown (15), followed by the transformation of t^6A to ms^2t^6A by the action of either CDKAL1/e-MtaB or YqeV/MtaB.

It is now well established that the MTTase enzymes that catalyze the methylthiolation reactions belong to a class of the radical AdoMet iron-sulfur enzyme family containing two [4Fe-4S] clusters. The enzymatic reaction proceeds through the following steps: (i) AdoMet reductive cleavage promoted by the radical AdoMet $[4Fe\text{-}4S]^{1+/2+}$ cluster to generate a 5′-deoxyadenosyl radical, Ado$^{\bullet}$; (ii) selective H atom abstraction at the substrate by Ado$^{\bullet}$; (iii) reaction of the resulting intermediate radical with a second $[4Fe\text{-}4S]^{1+/2+}$ cluster in the N-terminal UPF0004 domain, by an unknown mechanism, to generate a thiolated intermediate; and (iv) methylation at the introduced sulfur atom most probably through the reaction with the electrophilic methyl group of a second AdoMet molecule. The observation that YqeV/MtaB is able to bind two redox-active $[4Fe\text{-}4S]^{1+/2+}$ clusters is thus in full agreement with its involvement in a methylthiolation reaction.

To our knowledge five naturally occurring methylthio modifications have been reported so far; one of these occurs on a aspartic acid residue in ribosomal protein S12 and is

catalyzed by RimO family (4, 5). The other four all occur on the adenosine base found at position 37 adjacent to the 3′-end of the anticodon. This modification appears to be essential for efficient and highly accurate protein translation by the ribosome (13). The 2-methylthio-N^6-isopentenyladenosine (ms^2i^6A) is produced by the MTTase from the MiaB family (22). In this study, we demonstrate that the ms^2t^6A is produced by MTTases from either YqeV/MtaB or CDKAL1/e-MtaB families. There is as yet no experimental data establishing the identity of the enzymes catalyzing biosynthesis of 2-methylthio-N^6-hydroxynorvalyl-carbamoyladenosine (ms^2hn^6A) or the 2-methylthio-N^6-methyladenosine (ms^2m^6A). The occurrence of 2-methylthio-N^6-methyladenosine remains to be confirmed because only one organism (*Thermodesulfobacterium commune*, not yet completely sequenced) has been reported to contain this hypermodified base. The case of ms^2hn^6A is more intriguing. This base has been observed in *Thermotoga maritima* (26), which encodes three MTTases (MiaB, MtaB, and RimO, Fig. 1) but has been shown to contain four methylthiolated derivatives as follows: Asp-89 in ribosomal protein S12, ms^2i^6A, ms^2t^6A, and ms^2hn^6A (5, 26, 28). Based on the likelihood that all of methylthiolation reactions are catalyzed by radical AdoMet MTTases, there are two possible explanations for the generation of ms^2hn^6A. One possibility, as suggested previously (3), is that YqeV/MtaB family members have broad substrate specificity and can modify both t^6A and hn^6A bases, which differ only by the presence of an additional methyl group in hn^6A. Alternatively, a specific methylase could generate ms^2hn^6A from ms^2t^6A after production of this base by YqeV/MtaB. Further experiments are needed to distinguish between these possibilities.

The same methylthiolation reaction in tRNAs is catalyzed by different enzymes depending on the nature of the alkyl group at the N^6 of A-37. Interesting questions remain unanswered concerning the mechanism by which the active sites of MTTases control the selective recognition of the modified adenine 37 on tRNA substrates. Understanding these mechanisms will require the determination of the three-dimensional structure of enzymes such as MiaB, MtaB, and e-MtaB alone and in complex with their tRNA substrates.

Acknowledgments—We thank Jon D. Luff for bioinformatics support and Serge Gambarelli for providing EPR facilities. We thank the National BioResource Project (NIG, Japan) for generously providing the B. subtilis, wild-type (MGNA-A001), and yqeV- (MGNA-C496) strains. We also thank François Denizot for the generous gifts of pDG148-Stu plasmid. We are grateful to Dr. Jean-Michel Jault, Anne-Emmanuelle Foucher, and Maria-Halima Laaberki for helpful discussion about the manipulation of B. subtilis strains.

Addendum—During the submission process of this study, a closely related paper appeared in the literature (Anton, B. P., Russell, S. P., Vertrees, J., Kasif, S., Raleigh, E. A., Limbach, P. A., and Roberts, R. J. (2010) *Nucleic Acids Res.*, in press) that presents some results similar to ours on the *B. subtilis* YmcB/YqeV enzymes, in general agreement with our data. However, our study is substantially broader in the scope of both its bioinformatic and experimental analyses.

REFERENCES

1. Fontecave, M., Mulliez, E., and Atta, M. (2008) *Chem. Biol.* **15,** 209–210
2. Pierrel, F., Douki, T., Fontecave, M., and Atta, M. (2004) *J. Biol. Chem.* **279,** 47555–47563
3. Anton, B. P., Saleh, L., Benner, J. S., Raleigh, E. A., Kasif, S., and Roberts, R. J. (2008) *Proc. Natl. Acad. Sci. U.S.A.* **105,** 1826–1831
4. Lee, K. H., Saleh, L., Anton, B. P., Madinger, C. L., Benner, J. S., Iwig, D. F., Roberts, R. J., Krebs, C., and Booker, S. J. (2009) *Biochemistry* **48,** 10162–10174
5. Arragain, S., Garcia-Serres, R., Blondin, G., Douki, T., Clemancey, M., Latour, J. M., Forouhar, F., Neely, H., Montelione, G. T., Hunt, J. F., Mulliez, E., Fontecave, M., and Atta, M. (2010) *J. Biol. Chem.* **285,** 5792–5801
6. Hernández, H. L., Pierrel, F., Elleingand, E., García-Serres, R., Huynh, B. H., Johnson, M. K., Fontecave, M., and Atta, M. (2007) *Biochemistry* **46,** 5140–5147
7. Sofia, H. J., Chen, G., Hetzler, B. G., Reyes-Spindola, J. F., and Miller, N. E. (2001) *Nucleic Acids Res.* **29,** 1097–1106
8. Fontecave, M., Mulliez, E., and Ollagnier-de-Choudens, S. (2001) *Curr. Opin. Chem. Biol.* **5,** 506–511
9. Fontecave, M., Ollagnier-de-Choudens, S., and Mulliez, E. (2003) *Chem. Rev.* **103,** 2149–2166
10. Anantharaman, V., Koonin, E. V., and Aravind, L. (2001) *FEMS Microbiol. Lett.* **197,** 215–221
11. Durant, P. C., Bajji, A. C., Sundaram, M., Kumar, R. K., and Davis, D. R. (2005) *Biochemistry* **44,** 8078–8089
12. McCrate, N. E., Varner, M. E., Kim, K. I., and Nagan, M. C. (2006) *Nucleic Acids Res.* **34,** 5361–5368
13. Gustilo, E. M., Vendeix, F. A., and Agris, P. F. (2008) *Curr. Opin. Microbiol.* **11,** 134–140
14. Elkins, B. N., and Keller, E. B. (1974) *Biochemistry* **13,** 4622–4628
15. El Yacoubi, B., Lyons, B., Cruz, Y., Reddy, R., Nordin, B., Agnelli, F., Williamson, J. R., Schimmel, P., Swairjo, M. A., and de Crécy-Lagard, V. (2009) *Nucleic Acids Res.* **37,** 2894–2909
16. Steinthorsdottir, V., Thorleifsson, G., Reynisdottir, I., Benediktsson, R., Jonsdottir, T., Walters, G. B., Styrkarsdottir, U., Gretarsdottir, S., Emilsson, V., Ghosh, S., Baker, A., Snorradottir, S., Bjarnason, H., Ng, M. C., Hansen, T., Bagger, Y., Wilensky, R. L., Reilly, M. P., Adeyemo, A., Chen, Y., Zhou, J., Gudnason, V., Chen, G., Huang, H., Lashley, K., Doumatey, A., So, W. Y., Ma, R. C., Andersen, G., Borch-Johnsen, K., Jorgensen, T., van Vliet-Ostaptchouk, J. V., Hofker, M. H., Wijmenga, C., Christiansen, C., Rader, D. J., Rotimi, C., Gurney, M., Chan, J. C., Pedersen, O., Sigurdsson, G., Gulcher, J. R., Thorsteinsdottir, U., Kong, A., and Stefansson, K. (2007) *Nat. Genet.* **39,** 770–775
17. Altschul, S. F., Madden, T. L., Schäffer, A. A., Zhang, J., Zhang, Z., Miller, W., and Lipman, D. J. (1997) *Nucleic Acids Res.* **25,** 3389–3402
18. Chenna, R., Sugawara, H., Koike, T., Lopez, R., Gibson, T. J., Higgins, D. G., and Thompson, J. D. (2003) *Nucleic Acids Res.* **31,** 3497–3500
19. Kumar, S., Tamura, K., and Nei, M. (2004) *Brief. Bioinformatics* **5,** 150–163
20. Joseph, P., Fantino, J. R., Herbaud, M. L., and Denizot, F. (2001) *FEMS Microbiol. Lett.* **205,** 91–97
21. Yang, M. M., Zhang, W. W., Bai, X. T., Li, H. X., and Cen, P. L. (2009) *Mol. Biol. Rep.* **37,** 2207–2213
22. Pierrel, F., Björk, G. R., Fontecave, M., and Atta, M. (2002) *J. Biol. Chem.* **277,** 13367–13370
23. Turgay, K., Hahn, J., Burghoorn, J., and Dubnau, D. (1998) *EMBO J.* **17,** 6730–6738
24. Gehrke, C. W., and Kuo, K. C. (1989) *J. Chromatogr.* **471,** 3–36
25. Fish, W. W. (1988) *Methods Enzymol.* **158,** 357–364
26. Reddy, D. M., Crain, P. F., Edmonds, C. G., Gupta, R., Hashizume, T., Stetter, K. O., Widdel, F., and McCloskey, J. A. (1992) *Nucleic Acids Res.* **20,** 5607–5615
27. Auxilien, S., Keith, G., Le Grice, S. F., and Darlix, J. L. (1999) *J. Biol. Chem.* **274,** 4412–4420
28. Pierrel, F., Hernandez, H. L., Johnson, M. K., Fontecave, M., and Atta, M. (2003) *J. Biol. Chem.* **278,** 29515–29524
29. Esberg, B., Leung, H. C., Tsui, H. C., Björk, G. R., and Winkler, M. E. (1999) *J. Bacteriol.* **181,** 7256–7265
30. Tabor, S., and Richardson, C. C. (1985) *Proc. Natl. Acad. Sci. U.S.A.* **82,** 1074–1078

Brain Tumor Pathol (2011) 28:13–24
DOI 10.1007/s10014-010-0007-z

REVIEW ARTICLE

Angiogenesis and invasion in glioma

Manabu Onishi · Tomotsugu Ichikawa · Kazuhiko Kurozumi · Isao Date

Received: 20 July 2010 / Accepted: 22 September 2010 / Published online: 8 January 2011

Abstract Despite advances in surgical and medical therapy, glioblastoma consistently remains a fatal disease. Over the last 20 years, no significant increase in survival has been achieved for patients with this disease. The formation of abnormal tumor vasculature and glioma cell invasion along white matter tracts are believed to be the major factors responsible for the resistance of these tumors to treatment. Therefore, investigation of angiogenesis and invasion in glioblastoma is essential for the development of a curative therapy. In our report, we first reviewed certain histopathological studies that focus on angiogenesis and invasion of human malignant gliomas. Second, we considered several animal models of glioma available for studying angiogenesis and invasion, including our novel animal models. Third, we focused on the molecular aspects of glioma angiogenesis and invasion, and the key mediators of these processes. Finally, we discussed the recent and ongoing clinical trials targeting tumor angiogenesis and invasion in glioma patients. A better understanding of the mechanism of glioma angiogenesis and invasion will lead to the development of new treatment methods.

Keywords Glioma · Invasion · Angiogenesis · Hypoxia · Molecular targeted therapy

M. Onishi · T. Ichikawa (✉) · K. Kurozumi · I. Date
Department of Neurological Surgery,
Okayama University Graduate School of Medicine,
Dentistry and Pharmaceutical Sciences,
2-5-1, Shikata-cho, Kita-ku, Okayama 700-8558, Japan
e-mail: tomoichi@cc.okayama-u.ac.jp

M. Onishi
e-mail: onishi_manabu@yahoo.co.jp

Introduction

Despite advances in surgical and medical therapy, glioblastoma consistently remains a fatal disease. The pathophysiological processes of angiogenesis and tumor cell invasion play pivotal roles in glioma development and growth already in the earliest phase [1]. The formation of abnormal tumor vasculature and glioma cell invasion along white matter tracts are believed to be the major reasons for the resistance of these tumors to treatment. Recent insight into the fundamental processes governing glioma angiogenesis and invasion have provided renewed hope for developing novel strategies aimed at reducing morbidity due to this fatal disease. However, glioma angiogenesis and invasion are challenging to study in experimental settings because most of the animal models fail to mimic the unique angiogenesis and invasiveness of human glioma cells.

In this review, we first discuss the histopathological features of angiogenesis and invasion in human malignant glioma. Second, we considered several animal glioma models available for studying angiogenesis and invasion. We then focus our attention on the molecular biology of glioma angiogenesis and invasion, examining the key mediators of these processes. Lastly, we briefly discuss the recent and ongoing clinical trials targeting mediators of angiogenesis or invasion in glioma patients.

Histopathological studies of glioma angiogenesis and invasion

Glial tumors are believed to arise from neuroepithelial tissue and can be classified into astrocytic, oligodendroglial, and oligoastrocytic tumors. According to the World Health Organization (WHO), astrocytomas are classified

into four grades (I–IV) based on the histopathological features that correlate with prognosis [2]. Grade I tumors (pilocytic astrocytomas) are rare and biologically benign. Grade II tumors display nuclear atypia, and the median survival of patients with this tumor type is approximately 10 years. The median survival of patients with tumors classified as grade III (anaplastic astrocytoma) is approximately 2 years. Grade IV tumors, also called glioblastoma multiforme (GBM), have a very poor prognosis, and the median survival of patients with GBM is approximately 14.6 months [3]. Glioblastoma, the most malignant tumor among the astrocytic gliomas, is the most common primary brain tumor in adults.

Malignant glioma (WHO grade III and IV) occurs most often in the subcortical white matter of the cerebral hemispheres. Many reports have described the histopathological features of malignant gliomas. Marked proliferation, angiogenesis, and invasion have been recognized as hallmarks of this disease. Proliferation activity is usually prominent, with detectable mitoses present in nearly every case. Vascular proliferation is seen throughout the lesion, often around necrotic foci and in the peripheral infiltration zone. Glioblastomas are among the most vascularized human tumors [4]. Tumor infiltration often extends into the adjacent cortex and through the corpus callosum into the contralateral hemisphere.

Histopathological analysis of angiogenesis

Neovascularization in and around the malignant glioma is well recognized. Glioblastomas, one of the most well-studied tumor types, with regard to angiogenesis, are known to have blood vessels of increased diameter with high permeability, thickened basement membranes, and highly proliferative endothelial cells [5]. The presence of microvascular proliferation with the formation of glomerular capillary loops in garland-like formation [6] is a histopathological hallmark of glioblastoma. Increased neoplastic proliferation of glial cells running parallel to endothelial vascular proliferation is one of the malignancy evaluation criteria [7]. Vascular density in glioblastoma is markedly higher than that in tumors of lower histological grade [8]. An increase in vascularization significantly worsens prognosis [7]. Necrotic foci surrounded by pseudopalisading cells are a configuration relatively unique to glioblastoma. Recently, Rong et al. [9] demonstrated that pseudopalisading cells are present in severely hypoxic states and they overexpress hypoxia-inducible factor (HIF-1) and secreting proangiogenic factors, such as VEGF and IL-8. Thus, microvascular hyperplasia in glioblastoma, which provides a new vasculature and promotes peripheral tumor extension, is closely linked to the appearance of pseudopalisades.

Histopathological analysis of invasion

Although infiltrative spread is a common feature of all diffuse astrocytic tumors, glioblastoma is particularly infamous for its rapid invasion into neighboring brain structures [10]. Supratentorial bilateral extension occurs because of rapid growth along myelinated structures, in particular across the corpus callosum and along the fornices toward the temporal lobes. Extension within and along perivascular spaces is another typical mode of infiltration [11].

Magnetic resonance imaging (MRI) is frequently used to evaluate tumor vasculature and invasion [12]. In human glioma patients, only the central leaky part of high-grade gliomas can be visualized by gadolinium contrast enhancement, whereas the other outer rims of the tumor and infiltrating cells in the normal surrounding brain tissue, which are protected by normal vasculature, are not visible. The diffuse invasive area around the enhanced mass of a malignant glioma is depicted as high-intensity signals on T2-weighted images [13]. Although MRI is a powerful tool for high resolution in vivo imaging, sub-millimeter lesions are not always detected by MRI.

While histopathological studies have given insight into tumor invasion, there are limitations to this methodology. Several problems have been encountered in investigating glioma invasion, the most critical being the lack of glioma-specific antibodies for immunohistochemical analysis. Exact localization of invading glioma cells within seemingly normal brain parenchyma is crucial for the precise evaluation of invasion patterns. Recently, MAP2e, a splice variant of MAP2 (microtubule-associated protein), was reported as a candidate glioma-specific antigen. Most cells in CNS tumors, particularly oligodendrogliomas and glioblastomas, stain positively for MAP2e. Immunohistochemistry targeting MAP2e can therefore localize invasive glioma cells [14].

We examined samples of human glioblastomas by dual immunohistochemical staining with glioma- and endothelial-specific antibodies (MAP2e and vWf; von Willebrand factor, respectively), and examined the relationship between angiogenesis and invasion (Fig. 1). Our findings confirmed that there are at least two angiogenic and invasive glioma phenotypes. Clusters of glioma cells were seen around newly developed vessels in the normal parenchyma adjacent to the tumor margins. Single cell infiltrations into normal brain parenchyma independent of vasculature were also seen. These different invasive and angiogenic phenotypes are called angiogenesis-dependent and angiogenesis-independent invasions [15]. Malignant astrocytoma and glioblastoma consist of a mixture of subclones with both angiogenesis-dependent and angiogenesis-independent invasion phenotypes present in various proportions.

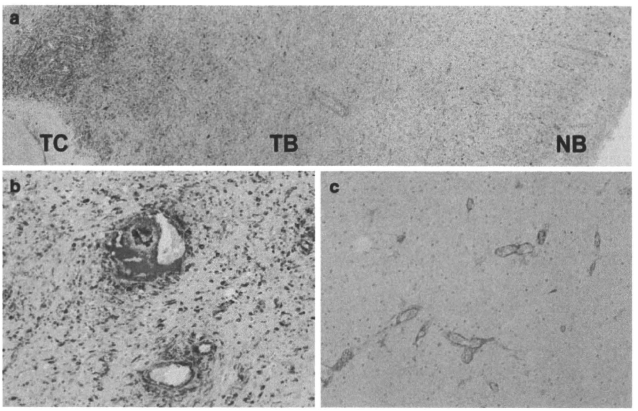

Fig. 1 MAP2e and vWf immunohistochemical staining of a human glioblastoma sample showing two distinct invasive and angiogenic phenotypes. Macroscopic appearance of glioblastoma sample (**a**). All tumor cells were positive for MAP2e and represented the diffuse infiltration from the tumor core (TC) to surrounding normal brain (NB) and thereby the absence of a border between tumor and normal brain (**a**). The center of the tumor showed high tumor cell density, endothelial proliferation, necrosis, and pseudopalisading of tumor cells around the necrotic focus. At the tumor border (TB), clusters of MAP2e-positive tumor cells were observed around dilated vessels (**b**). In normal brain (NB) tissues where no dilated vessels were observed, single MAP2e-positive tumor cells were diffusely distributed (**c**). MAP2e: DAB, vWf: DAB-Ni, counterstain: hematoxylin. *TC* tumor core, *TB* tumor border, *NB* normal brain

Moreover, gliomatosis cerebri is an extreme example of a tumor that consists solely of subclones with an angiogenesis-independent invasion phenotype.

Animal models for studying glioma invasion and angiogenesis

To study the histopathological and molecular bases of malignant glioma, several animal models of glioma have been established by intracerebral inoculation of highly proliferative glioma cells in culture. Glioma invasion and angiogenesis are challenging areas to study because most traditional animal models do not recapitulate the unique features of invasiveness and angiogenesis of human glioma cells [16]. Typically, such transplantable tumors in mice or rats form solid nodules at the injection site, which compress rather than invade the surrounding brain regions. Recently, several new glioma models have been developed, which replicate the invasive behavior and show neovascularization. In particular, some sophisticated animal models exist in which human glioma xenografts can show various degrees of true invasion. These models include (1) direct implantation of patient surgical specimens into the brains of nude mice [17], (2) transplantation of patient surgical material s.c. in nude mice followed by dissociation and orthotopic reinjection of these xenotransplants [18], (3) engraftment of glioblastoma-derived spheroids after short-term culture into rat brain [19], and (4) engraftment of glioblastoma stem cell-enriched cultures into mouse brain [20, 21]. Although these models are reproducible, they require some special procedures to develop the brain tumors, such as in vivo preparation of xenografts or in vitro spheroid formation before implantation.

We have developed a pair of glioma cell lines that show different invasive and angiogenic behaviors in the brains of immunocompromised animals (S. Inoue, T. Ichikawa, T. Maruo et al. Novel animal glioma models that separately exhibit two different invasive and angiogenic phenotypes of human glioblastomas; submitted). Histopathologically, one shows angiogenesis-dependent invasion with cluster formation around neovascular vessels in the tumor margin, and the other shows single cell infiltration into the normal brain parenchyma without angiogenesis (Fig. 2). These animal glioma models separately mimic the two phenotypes of human glioblastoma invasion: angiogenesis-dependent and angiogenesis-independent invasions. Our models can be readily established without any complicated cell preparation, and they give steady reproducibility of tumor development with the same phenotypic growth as that observed in human glioma. These novel models would be particularly beneficial for analyzing the molecular mechanisms of invasion and angiogenesis in glioma and investigation of new therapies for glioma.

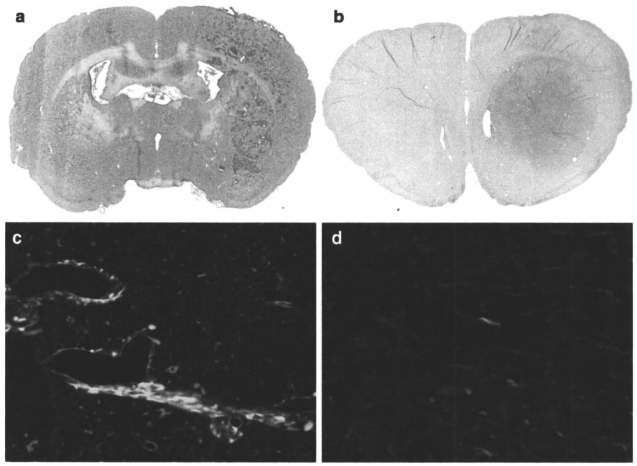

Fig. 2 Two animal brain tumor models showing distinct phenotypes of invasion. J3T-1 brain tumor established in athymic rat brain (**a**). J3T-1 cells formed well-demarcated and highly angiogenic tumors in the rat brain. Clusters of tumor cells were seen around newly developed vessels in adjacent normal brain. J3T-1G cells expressing green fluorescent protein (GFP) coopting around dilated vessels (*red*) (**c**). J3T-2 brain tumor established in athymic rat brain (**b**). J3T-2 cells formed poorly demarcated tumors with tumor cells gradually dispersed from the tumor center to the normal brain parenchyma. J3T-2G single cells diffusely invaded normal brain tissue (**d**). **a**, **b** H&E staining. **c**, **d** Tumor cell (GFP, *green*), vascular stain (RECA-1, *red*), nuclear stain (DAPI, *blue*)

Molecular biology of angiogenesis in glioma

Angiogenesis is a key event in the progression of malignant gliomas. The presence of microvascular proliferation leads to the histological diagnosis of GBM [22]. Among all solid tumors, GBM has been reported to be the most angiogenic by displaying the highest degree of vascular proliferation and endothelial cell hyperplasia [23]. Such intense vascularization might be responsible for the peritumoral edema, one of the pathological features of GBM [24, 25].

Angiogenesis is the formation of new blood vessels by rerouting or remodeling of existing vessels, and it is believed to be the primary method of vessel formation in gliomas. Angiogenesis requires three distinct steps: (1) blood vessel breakdown, (2) degradation of the vessel basement membrane and surrounding extracellular matrix (ECM), and (3) migration of endothelial cells and the formation of new blood vessels (Fig. 3).

Blood vessel breakdown

The first step in forming new blood vessels from existing vessels is the dissolution of aspects of native vessels. Glioma cells first accumulate around the existing cerebral blood vessels and lift off the astrocytic foot processes, which leads to the disruption of the normal contact between endothelial cells and the basement membrane [26]. The affected endothelial cells express angiopoietin-2 (Ang-2), resulting in destabilization of the vessel wall and decreased pericyte coverage [26–28]. Ang-1 and -2 are important endothelial growth factors that signal via the Tie2 receptor tyrosine kinase (RTK) expressed on endothelial cells. In the normal brain, Ang-1 binds to Tie2 to induce association between pericytes and endothelial cells, resulting in stabilization of the vasculature [29, 30]. On the other hand, Ang-2 may act as an antagonist to Tie2 phosphorylation, leading to destabilization of blood vessels. Therefore, Ang-2 represents a checkpoint for Ang-1/Tie2-mediated angiogenesis [26, 31].

Degradation of the vessel basement membrane and surrounding ECM

Degradation of the vessel basement membrane and surrounding ECM, which also facilitates the invasion of endothelial cells, is an integral part of the ongoing angiogenic process [32]. The matrix metalloproteinase (MMP) family enzymes that degrade components of ECM consist of four groups according to their substrates: collagenases, gelatinases, stromelysins, and membrane-associated MMPs.

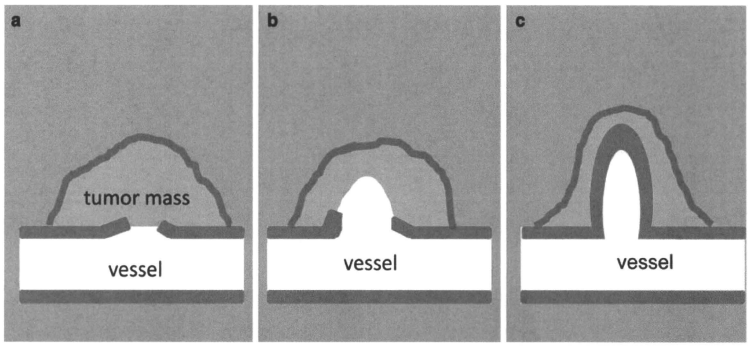

Fig. 3 Schematic representation of the mechanism of angiogenesis in glioma. Angiogenesis requires three distinct steps: (**a**) blood vessel breakdown, (**b**) degradation of the vessel basement membrane and surrounding ECM, and (**c**) migration of endothelial cells and formation of new blood vessels

Gelatinases-A (MMP-2) and gelatinases-B (MMP-9) are highly expressed in astrocytomas, and their expression levels, especially those of MMP-9, correlate with the histological grade of tumor. Both MMP-2 and MMP-9 have been detected in blood vessels as well as in tumor cells [33, 34]. MMP-2 and MMP-9 expression is strongly induced by hypoxia, and these two molecules appear to have a synergistic effect on basement membrane degradation [35].

Migration of endothelial cells and formation of new blood vessels

After regression of existing vessels and breakdown of the basement membrane, endothelial cells proliferate and migrate toward the tumor cells expressing pro-angiogenic compounds. Integrin $\alpha v\beta 3$ and $\alpha 5\beta 1$ are upregulated in endothelial cells during angiogenesis, enhancing endothelial cell adhesion and migration [36, 37]. In addition to migration of endothelial cells, migration of pericytes is an important part of tumor vessel formation. Platelet-derived growth factor (PDGF) secretion by activated endothelial cells recruits pericytes to the site of newly sprouting vessels and aids in establishing a new basement membrane [38, 39].

Hypoxia and angiogenesis

Vascular homeostasis is governed by a balance between pro-angiogenic and anti-angiogenic stimuli [40]. Angiogenesis is activated in growing gliomas when the pro-angiogenic stimuli outweigh the anti-angiogenic stimuli. The most potent activator of angiogenic mechanisms in brain tumors is tissue hypoxia. One well-studied pathway is the HIF-1/VEGF-A pathway, which leads to endothelial cell proliferation and migration [41]. The transcription factor HIF-1, which is composed of two subunits, HIF-1β, and HIF-1α, is the classic and best-characterized hypoxia-regulated molecule. Interestingly, HIF-1β remains unchanged under hypoxic conditions. However, at the posttranscriptional level, HIF-1α protein is upregulated under hypoxic (1–2% O_2) conditions [42]. Under these conditions, HIF-1 activates DNA promoter regions known as hypoxia response elements (HREs). HREs induce transcription of >100 genes that help the cell cope with low O_2 conditions [43, 44]. VEGF, which regulates tumor edema and blood vessel formation, is an example of a gene regulated by an HIF-1 though an HRE. Specifically, VEGF-A is known to be upregulated in glioblastoma and is produced by multiple cell types, including tumor, stromal, and inflammatory cells [45]. VEGF-A binds to two RTKs (receptor; tyrosine kinases), VEGFR-1 (Flt-1) and VEGFR-2 (KDR, Flk-1) [46]. VEGF-A regulates endothelial cell survival, proliferation, permeability, and migration primarily via VEGF-receptor 2 (VEGFR2) [47]. VEGF promotes endothelial proliferation via activation of the MAPK pathway [22]. VEGF also enhances vascular permeability through the MAPK signaling cascade by rearranging cadherin/catenin complexes and loosening adhering junctions between endothelial cells [48, 49]. VEGF stimulates endothelial production of urokinase-type plasminogen activator (uPA) [50], which induces conversion of plasminogen to plasmin, causing the breakdown of ECM components and leading to ECM remodeling [22]. The end result of VEGF signaling in tumors is the production of immature, highly permeable blood vessels with subsequent poor maintenance of BBB and parenchymal edema [40, 51].

Molecular biology of glioma invasion

One of the insidious features of gliomas is the potential of single cells to invade normal brain tissue, blurring tumor margins, and establishing numerous microtumors at a distance from the primary tumor. The detailed mechanisms of glioma invasion are only beginning to be understood.

Invasion of tumor cells into normal tissue is thought to be a multifactorial process, consisting of cell interactions with ECM and with adjacent cells, as well as accompanying biochemical processes supportive of active cell movement. It is well known that cell motility is not a de novo feature that emerges coincident to carcinogenesis. Several cell types exhibit active movement during various stages of embryonal development, during wound healing, and in the course of immune responses. This motile behavior is regulated in a very rigid manner, suggesting that the reappearance of a motile phenotype in cancer cells results from the loss or cessation of normal inhibitory controls [52, 53]. Many have proposed that the highly infiltrative nature of human gliomas recapitulates the migratory behavior of glial progenitors [14, 54, 55].

Tumor cell invasion requires four distinct steps: (1) detachment of invading cells from the primary tumor mass, (2) adhesion to ECM, (3) degradation of ECM, and (4) cell motility and contractility (Fig. 4).

Detachment of invading cells from the primary tumor mass

The detachment of invading glioma cells from the primary tumor mass involves several events. The first event entails destabilization and disorganization of cadherin-mediated junctions that hold the primary mass together. Cadherins (E-, P-, and N-cadherin) form adherent junctions, which are calcium-dependent, transmembrane, cell–cell adhesion complexes. Due to their contribution to processes such as morphological differentiation and contact inhibition of growth and motility, cadherins may function as suppressors of tumor growth and invasion [53]. During carcinoma progression, decreased cadherin function is correlated with de-differentiation, metastasis, and poor prognosis [56].

The second event is a decline in the expression of connexin 43, which leads to a reduction in gap junction formation. Cell–cell communication is important in growth control and differentiation, and it is partly achieved using gap junctions and via second messengers [57]. Decreased gap junction formation may result in fewer inhibitory signals, facilitating uncontrolled cell division and de-differentiation [58]. Connexin 43 is the most abundant gap junction protein in CNS and is expressed primarily in astrocytes [59]. McDonough and coworkers [60] have reported that reduced gap junction formation is correlated with increased motility of glioma cells in vitro. Increased malignancy of glioma specimens correlates with reduced in situ gap junction formation as well as reduced connexin 43 expression [61]. These observations suggest that decreased expression of connexin 43 is important for increased growth and invasion of gliomas [53].

The third event is cleavage of CD44, which anchors the primary mass to ECM, by the metalloproteinase ADAM. CD44 is a transmembrane glycoprotein belonging to the immunoglobulin receptor superfamily, which interacts with hyaluronic acid as its ligand. Hyaluronic acid comprises a substantial fraction of brain ECM and is implicated in a wide variety of physiological and pathological

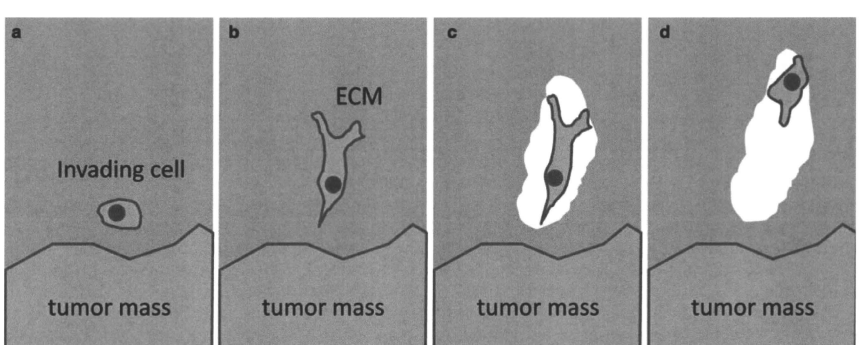

Fig. 4 Schematic representation of the mechanism of glioma invasion. Invasion requires four distinct steps: (**a**) detachment of invading cells from the primary tumor mass, (**b**) adhesion to ECM, (**c**) degradation of ECM, and (**d**) cell motility and contractility

processes [62]. Monoclonal antibodies directed against CD44 decrease intracerebral invasion of glioma cells in vivo and through matrigel matrices in vitro [63]. CD44 can be cleaved by ADAM 10 and 17, and both the extracellular and intracellular cleaved components of CD44 promote cell migration [64].

Adhesion to ECM

The most common molecules that allow glioma cells to adhere to ECM are the integrins. Integrins are transmembrane glycoproteins composed of two subunits (α and β). They interact with two large groups of ligands: a variety of ECM proteins, such as fibronectin, vitronectin, fibrinogen, and cell surface molecules, that are members of the immunoglobulin supergene family, such as intracellular adhesion molecules (ICAM-1, ICAM-2) and vascular cell adhesion molecule (VCAM-1). In particular, the integrin $\alpha v\beta 3$, which binds to fibronectin, vitronectin, and tenascin-C in ECM, is thought to play a central role in glioma invasion [65]. Increased expression of integrin $\alpha v\beta 3$ leads to increased motility in human glioma cells with a concomitant decrease in apoptosis sensitivity. Conversely, inhibition of integrin $\alpha v\beta 3$ decreases glioma cell motility [66]. Several factors expressed in glioma cells have been found to regulate integrin expression. Particularly, uPA secreted by glioma cells has been shown to upregulate integrin $\alpha v\beta 3$ expression by autocrine mechanism [67]. Glioma expression of focal adhesion kinase, a nonreceptor cytoplasmic tyrosine kinase, has been shown to increase phosphorylation of the enhancer of filamentation 1, which in turn stimulates PDGF-mediated stimulation of glioma integrin adhesion to ECM [68].

Degradation of ECM

The most common proteases that degrade ECM to create the space for invading glioma cells are MMPs. The first experimental evidence for a role of MMPs in tumor development was obtained in the early 1980s when a type IV collagenase was demonstrated to be involved in melanoma invasion and metastasis [69]. Wild-Bode et al. [70] found that MMP-2 and MMP-3 levels and MMP-2/MMP-9 activity correlated with glioma cell migration and invasion. Regulation of MMP-2 and MMP-9, the most frequently expressed glioma invasion-mediating factors, has been extensively studied. NF-κB, uPA, low-density lipoprotein receptor-related protein 1, and insulin-like growth factor binding protein-2 are known to upregulate MMP expression [71–73]. Induced expression of tissue inhibitor of metalloproteinases-3 (TIMP-3), a putative inhibitor of MMP activity, has been shown to suppress infiltration and also to induce apoptosis in cancer cell lines [74]. Similarly, several MMP inhibitors have been observed to effectively downregulate glioma invasion in vitro [75, 76].

Cell motility and contractility

Cell motility requires cytoplasmic contractile force. Glioma cells migrate similarly to nontransformed neural progenitor cells, extending a prominent leading cytoplasmic process followed by a burst of forward movement in the cell body. As is the case with neural progenitor cells, glioma motility and contractility require A and B isoforms of myosin II. Myosin II is the major source of cytoplasmic contractile force. Myosin II allows glioma cells to squeeze through pores smaller than their nuclear diameter, which is important because the brain has particularly narrow extracellular spaces [77]. The activity of myosin II is controlled by phosphorylation of a serine residue on its regulatory light chain (RLC). Phosphorylation of RLC by myosin light chain kinase (MLCK) activates myosin II. This action is opposed by dephosphorylation of RLC, which is mediated by a specific MLC (myosin light chain) phosphatase. Thus, the degree of activity of myosin II in a cell is controlled by the relative balance of activities of MLCK and MLC phosphatase. Small GTPases, such as RhoA, Rac, cdc42, as well as RLC-interacting protein, are also involved in this process in glioma cells [78, 79].

Hypoxia and glioma invasion

In studies of human GBM surgical specimens, pseudopalisading cells found in the necrotic areas are known to be hypoxic, as demonstrated by their dramatic upregulation of HIF-1, a nuclear transcription factor that orchestrates the adaptive response of the cells to lower oxygen [9, 80, 81]. Therefore, the pseudopalisading cells have been implicated in hypoxia-regulated migration away from these necrotic regions [82]. Limitations in oxygen diffusion would cause tumor cells at the furthermost distance from arterial supplies to became hypoxic and migrate towards viable vessels [82]. This is further supported by both in vitro and in vivo models, suggesting that tumor hypoxia results in increased GBM cell migration and, presumably, also invasion [83].

A significant number of human GBMs respond to hypoxia with an induction of c-Met, which is the receptor for scatter factor (SF)/hepatocyte growth factor (HGF). When hypoxia stimulates tumor cells to activate the c-met/SF/HGF pathway, c-met stimulates glioma cells to secrete uPA, which converts the circulating plasminogen into plasmin. Then plasmin degrades a variety of ECM proteins and activates several MMPs, which help glioma cells to invade the surrounding tissue [84, 85].

Molecular targeted therapy for glioma angiogenesis and invasion

Despite the genetic heterogeneity of malignant gliomas, common aberrations exist in the signaling elements of their angiogenesis and invasion pathways. New treatments have emerged to target molecules in these signaling pathways with the goal of clinical efficacy and minimal toxicity. Here, we review several clinical trials of new therapies that target the molecular mediators of glioma angiogenesis and invasion.

Bevacizumab

Bevacizumab, a humanized neutralizing monoclonal antibody against VEGF, has demonstrated encouraging radiographic responses in patients with recurrent malignant gliomas in combination with irinotecan [86]. Although a significant antitumor effect was observed in this phase II trial with a 63% radiographic response, the 6-month progression-free survival, which is a more positive primary endpoint for phase II trials in malignant gliomas, was 32% for GBM [87]. Recent data concerning the clinical use of anti-angiogenic drugs for recurrent malignant gliomas have been disappointing [88]. Some patients treated with bevacizumab have shown a reduction in the Gd-enhanced tumor size, but significant increases in the volume of infiltrative tumor relative to the enhanced tumor were also observed. Indeed, an experimental study showed that anti-angiogenic therapy of murine gliomas with an antibody against VEGF-R2 caused small satellite tumors to arise near the primary mass, centered around core vessels, akin to the perivascular invasion found more recently in the VEGF knockout glioma cell lines described previously [89]. Further research will be needed to identify mediators of this invasion and to determine whether the invasion seen after bevacizumab treatment of human glioblastomas is the perivascular invasion seen in the murine cell lines or the parenchymal type of invasion along white matter typically seen in glioblastomas [1]. One recent clinical trial suggested that the presence of tumor hypoxia markers predicts radiographic response and survival of patients treated with bevacizumab and irinotecan [90].

It has been proposed that hypoxia caused by vessel regression during the course of anti-angiogenic therapy leads to upregulation of proangiogenic factors and recruitment of bone marrow-derived cells (BMDCs) that have the capacity to increase tumor growth by means of new blood vessel growth [91]. Glioma cells evade antiangiogenic therapies by upregulating alternative proangiogenic signal circuits, including those utilizing fibroblast growth factor, ephrin A1, and angiopoietin 1. Another adaptive measure is the hypoxia-regulated recruitment of vascular progenitor cells and proangiogenic monocytes from the bone marrow to tumors [91].

Cilengitide

Integrins, cell adhesion molecules, play an important role in both glioma cell migration and angiogenesis. Cilengitide, an intravenous inhibitor of $\alpha v\beta 3$ and $\alpha v\beta 5$ integrins, demonstrated efficacy against an animal malignant glioma model [92]. Blocking $\alpha v\beta 3$ integrin inhibits blood vessel formation in vivo [93]. Cilengitide induces apoptosis in U87 glioma cells by preventing adherence to vitronectin and tenascin, matrix protein mediators of brain tumor invasion, and growth [94]. A phase I clinical trial of cilengitide in recurrent malignant gliomas by the New Approaches to Brain Tumor Therapy (NABTT) has been completed with no dose-limiting toxicities [95]. The most notable trial to date was a randomized phase II study of cilengitide, which was associated with a median survival of 10 months in recurrent glioma patients [96]. The North American Brain Tumor Consortium (NABTC) study was designed to determine whether cilengitide effectively penetrates into GBM in human patients. This study confirmed that cilengitide is effectively delivered into primary human GBM tumors with good retention. Recently, phase II studies of cilengitide in newly diagnosed GBM patients were presented. Patients with lowered MGMT expression based on gene promoter methylation appeared to benefit more with the addition of cilengitide [97]. The effect of combination therapy, such as cilengitide with XRT or with another chemotherapeutic agent, is likely to be cumulative.

Marimastat

Increased MMP levels are associated with glioma invasion and angiogenesis. Marimastat (MT), an orally active drug, can reduce MMP levels in patients with gliomas [98]. One phase II study evaluated MT combined with temozolomide (TMZ) in patients with recurrent malignant glioma [99]. For all patients, the progression-free survival (PFS) at 6 months was 39%. Median PFS was 17 weeks, median overall survival was 45 weeks, and 12-month PFS was 16%. A good outcome was documented, but joint and tendon pain was reported in 47% of patients. Eleven percent of patients were removed from the study because of intolerable joint pain. Further investigation of therapy-induced joint pain is needed.

Thalidomide

Thalidomide is an immunomodulatory agent that inhibits angiogenesis [100]. While thalidomide's anti-angiogenic mechanism is not understood, it has been suggested to

interfere with the expression of integrin receptors $\alpha v\beta 3$ and $\alpha v\beta 5$ and also to inhibit VEGF [101]. While thalidomide proved to be unsuccessful when used as a monotherapy in GBM, the measured response rate was 6%, and the 12-month overall survival was 22% [102].

Sorafenib

Sorafenib is a multikinase inhibitor, and inhibits Raf, VEGF, PDGFR-b, and c-Kit. Sorafenib suppresses angiogenesis via inhibition of VEGFR and PDGFR activities in endothelial cells [103]. Sorafenib-treated mice showed significant inhibition of glioblastoma cell proliferation, increased apoptosis and autophagy, and suppression of angiogenesis in vivo [104]. Phase II trials of sorafenib in patients with malignant gliomas are ongoing [22].

Imatinib

Imatinib is a kinase inhibitor of PDGFR, c-kit, and bcr-abl. PDGF and its cognate receptors, PDGFR, are important in growth and angiogenesis of glioma [105]. The in vitro effects of imatinib on glioma cell proliferation have been investigated. Imatinib at low concentrations can act as a cytostatic agent, whereas at high concentrations it mainly behaves as a cytotoxic agent [106]. Imatinib monotherapy has failed to show any significant clinical benefits. There are several potential reasons for the disappointing results with imatinib monotherapy in malignant gliomas. The penetration of the drug across BBB is likely to be limited by P-glycoprotein and other efflux pumps, thus reducing tumor concentrations of the drug. A second reason for the limited activity of imatinib may be that inhibition of PDGFR alone is insufficient to prevent growth of malignant gliomas [107].

Tenascin-C immunotherapy

Tenascin-C has been identified in hyperplastic vessels and is found to promote migration of endothelial cells in astrocytic tumors [108, 109]. Therefore, targeting tenascin with an antibody to suppress angiogenesis seems biologically reasonable. A tenascin-specific antibody radiolabeled with I-131 was tested in patients with high-grade gliomas [110]. The phase II studies with I-131 in malignant glioma were reported to yield a slight increase in survival time [111].

Conclusion

The mechanisms of glioma angiogenesis and invasion are only just beginning to be investigated, and many aspects are yet to be clarified. A better understanding of the molecular components responsible for glioma angiogenesis and invasion will hopefully lead to the development of new treatment methods. We hope that our novel glioma model described in this review can contribute in this aspect.

References

1. Bello L, Giussani C, Carrabba G et al (2004) Angiogenesis and invasion in gliomas. Cancer Treat Res 117:263–284
2. Kleihues P, Louis DN, Scheithauer BW et al (2002) The WHO classification of tumors of the nervous system. J Neuropathol Exp Neurol 61:215–225 (discussion 26–29)
3. Stupp R, Mason WP, van den Bent MJ et al (2005) Radiotherapy plus concomitant and adjuvant temozolomide for glioblastoma. N Engl J Med 352:987–996
4. Plate KH, Risau W (1995) Angiogenesis in malignant gliomas. Glia 15:339–347
5. Lopes MB (2003) Angiogenesis in brain tumors. Microsc Res Tech 60:225–230
6. Reifenberger G, Collins VP (2004) Pathology and molecular genetics of astrocytic gliomas. J Mol Med 82:656–670
7. Lebelt A, Dzieciol J, Guzinska-Ustymowicz K et al (2008) Angiogenesis in gliomas. Folia Histochem Cytobiol 46:69–72
8. Wesseling P, Ruiter DJ, Burger PC (1997) Angiogenesis in brain tumors; pathobiological and clinical aspects. J Neurooncol 32:253–265
9. Rong Y, Durden DL, Van Meir EG et al (2006) 'Pseudopalisading' necrosis in glioblastoma: a familiar morphologic feature that links vascular pathology, hypoxia, and angiogenesis. J Neuropathol Exp Neurol 65:529–539
10. Cingolani A, De Luca A, Larocca LM et al (1998) Minimally invasive diagnosis of acquired immunodeficiency syndrome-related primary central nervous system lymphoma. J Natl Cancer Inst 90:364–369
11. Burger PC, Heinz ER, Shibata T et al (1988) Topographic anatomy and CT correlations in the untreated glioblastoma multiforme. J Neurosurg 68:698–704
12. Koutcher JA, Hu X, Xu S et al (2002) MRI of mouse models for gliomas shows similarities to humans and can be used to identify mice for preclinical trials. Neoplasia 4:480–485
13. Tovi M, Hartman M, Lilja A et al (1994) MR imaging in cerebral gliomas tissue component analysis in correlation with histopathology of whole-brain specimens. Acta Radiol 35:495–505
14. Suzuki SO, Kitai R, Llena J et al (2002) MAP-2e, a novel MAP-2 isoform, is expressed in gliomas and delineates tumor architecture and patterns of infiltration. J Neuropathol Exp Neurol 61:403–412
15. Sakariassen PO, Prestegarden L, Wang J et al (2006) Angiogenesis-independent tumor growth mediated by stem-like cancer cells. Proc Natl Acad Sci USA 103:16466–16471
16. Tate MC, Aghi MK (2009) Biology of angiogenesis and invasion in glioma. Neurotherapeutics 6:447–457
17. Horten BC, Basler GA, Shapiro WR (1981) Xenograft of human malignant glial tumors into brains of nude mice. A histopathological study. J Neuropathol Exp Neurol 40:493–511
18. Giannini C, Sarkaria JN, Saito A et al (2005) Patient tumor EGFR and PDGFRA gene amplifications retained in an invasive intracranial xenograft model of glioblastoma multiforme. Neuro Oncol 7:164–176

19. Engebraaten O, Fodstad O (1999) Site-specific experimental metastasis patterns of two human breast cancer cell lines in nude rats. Int J Cancer 82:219–225
20. Galli R, Binda E, Orfanelli U et al (2004) Isolation and characterization of tumorigenic, stem-like neural precursors from human glioblastoma. Cancer Res 64:7011–7021
21. Gunther HS, Schmidt NO, Phillips HS et al (2008) Glioblastoma-derived stem cell-enriched cultures form distinct subgroups according to molecular and phenotypic criteria. Oncogene 27:2897–2909
22. Wong ML, Prawira A, Kaye AH et al (2009) Tumour angiogenesis: its mechanism and therapeutic implications in malignant gliomas. J Clin Neurosci 16:1119–1130
23. Brem S, Cotran R, Folkman J (1972) Tumor angiogenesis: a quantitative method for histologic grading. J Natl Cancer Inst 48:347–356
24. Zagzag D, Goldenberg M, Brem S (1989) Angiogenesis and blood–brain barrier breakdown modulate CT contrast enhancement: an experimental study in a rabbit brain-tumor model. Am J Roentgenol 153:141–146
25. Del Maestro RF, Megyesi JF, Farrell CL (1990) Mechanisms of tumor-associated edema: a review. Can J Neurol Sci 17:177–183
26. Zagzag D, Amirnovin R, Greco MA et al (2000) Vascular apoptosis and involution in gliomas precede neovascularization: a novel concept for glioma growth and angiogenesis. Lab Invest 80:837–849
27. Holash J, Maisonpierre PC, Compton D et al (1999) Vessel cooption, regression, and growth in tumors mediated by angiopoietins and VEGF. Science 284:1994–1998
28. Zagzag D, Hooper A, Friedlander DR et al (1999) In situ expression of angiopoietins in astrocytomas identifies angiopoietin-2 as an early marker of tumor angiogenesis. Exp Neurol 159:391–400
29. Bergers G, Song S (2005) The role of pericytes in blood-vessel formation and maintenance. Neuro Oncol 7:452–464
30. Reiss Y, Machein MR, Plate KH (2005) The role of angiopoietins during angiogenesis in gliomas. Brain Pathol 15:311–317
31. Maisonpierre PC, Suri C, Jones PF et al (1997) Angiopoietin-2, a natural antagonist for Tie2 that disrupts in vivo angiogenesis. Science 277:55–60
32. Rooprai HK, McCormick D (1997) Proteases and their inhibitors in human brain tumours: a review. Anticancer Res 17:4151–4162
33. Rao JS, Yamamoto M, Mohaman S et al (1996) Expression and localization of 92 kDa type IV collagenase/gelatinase B (MMP-9) in human gliomas. Clin Exp Metastasis 14:12–18
34. Forsyth PA, Wong H, Laing TD et al (1999) Gelatinase-A (MMP-2), gelatinase-B (MMP-9) and membrane type matrix metalloproteinase-1 (MT1-MMP) are involved in different aspects of the pathophysiology of malignant gliomas. Br J Cancer 79:1828–1835
35. Lakka SS, Gondi CS, Rao JS (2005) Proteases and glioma angiogenesis. Brain Pathol 15:327–341
36. Brooks PC, Clark RA, Cheresh DA (1994) Requirement of vascular integrin alpha v beta 3 for angiogenesis. Science 264:569–571
37. Kim S, Bell K, Mousa SA et al (2000) Regulation of angiogenesis in vivo by ligation of integrin alpha5beta1 with the central cell-binding domain of fibronectin. Am J Pathol 156:1345–1362
38. Lindahl P, Johansson BR, Leveen P et al (1997) Pericyte loss and microaneurysm formation in PDGF-B-deficient mice. Science 277:242–245
39. Ferrara N, Kerbel RS (2005) Angiogenesis as a therapeutic target. Nature 438:967–974
40. Jain RK, di Tomaso E, Duda DG et al (2007) Angiogenesis in brain tumours. Nat Rev Neurosci 8:610–622
41. Safran M, Kaelin WG Jr (2003) HIF hydroxylation and the mammalian oxygen-sensing pathway. J Clin Invest 111:779–783
42. Jiang BH, Rue E, Wang GL et al (1996) Dimerization, DNA binding, and transactivation properties of hypoxia-inducible factor 1. J Biol Chem 271:17771–17778
43. Wenger RH, Stiehl DP, Camenisch G (2005) Integration of oxygen signaling at the consensus HRE. Sci STKE 2005:re12
44. Brahimi-Horn C, Berra E, Pouyssegur J (2001) Hypoxia: the tumor's gateway to progression along the angiogenic pathway. Trends Cell Biol 11:S32–S36
45. Hanahan D, Folkman J (1996) Patterns and emerging mechanisms of the angiogenic switch during tumorigenesis. Cell 86:353–364
46. Ferrara N (2004) Vascular endothelial growth factor: basic science and clinical progress. Endocr Rev 25:581–611
47. Carmeliet P, Jain RK (2000) Angiogenesis in cancer and other diseases. Nature 407:249–257
48. Esser S, Lampugnani MG, Corada M et al (1998) Vascular endothelial growth factor induces VE-cadherin tyrosine phosphorylation in endothelial cells. J Cell Sci 111(Pt 13):1853–1865
49. Kevil CG, Payne DK, Mire E et al (1998) Vascular permeability factor/vascular endothelial cell growth factor-mediated permeability occurs through disorganization of endothelial junctional proteins. J Biol Chem 273:15099–15103
50. Mandriota SJ, Seghezzi G, Vassalli JD et al (1995) Vascular endothelial growth factor increases urokinase receptor expression in vascular endothelial cells. J Biol Chem 270:9709–9716
51. Jain RK (2003) Molecular regulation of vessel maturation. Nat Med 9:685–693
52. Graham CH, Connelly I, MacDougall JR et al (1994) Resistance of malignant trophoblast cells to both the anti-proliferative and anti-invasive effects of transforming growth factor-beta. Exp Cell Res 214:93–99
53. Demuth T, Berens ME (2004) Molecular mechanisms of glioma cell migration and invasion. J Neurooncol 70:217–228
54. Dirks PB (2001) Glioma migration: clues from the biology of neural progenitor cells and embryonic CNS cell migration. J Neurooncol 53:203–212
55. Farin PW, Crosier AE, Farin CE (2001) Influence of in vitro systems on embryo survival and fetal development in cattle. Theriogenology 55:151–170
56. Bremnes RM, Veve R, Hirsch FR et al (2002) The E-cadherin cell–cell adhesion complex and lung cancer invasion, metastasis, and prognosis. Lung Cancer 36:115–124
57. Goodenough DA, Goliger JA, Paul DL (1996) Connexins, connexons, and intercellular communication. Annu Rev Biochem 65:475–502
58. Ruch RJ (1994) The role of gap junctional intercellular communication in neoplasia. Ann Clin Lab Sci 24:216–231
59. Dermietzel R, Spray DC (1993) Gap junctions in the brain: where, what type, how many and why? Trends Neurosci 16:186–192
60. McDonough WS, Johansson A, Joffee H et al (1999) Gap junction intercellular communication in gliomas is inversely related to cell motility. Int J Dev Neurosci 17:601–611
61. Soroceanu L, Manning TJ Jr, Sontheimer H (2001) Reduced expression of connexin-43 and functional gap junction coupling in human gliomas. Glia 33:107–117
62. Nagano O, Saya H (2004) Mechanism and biological significance of CD44 cleavage. Cancer Sci 95:930–935
63. Gunia S, Hussein S, Radu DL et al (1999) CD44s-targeted treatment with monoclonal antibody blocks intracerebral invasion and growth of 9L gliosarcoma. Clin Exp Metastasis 17:221–230

64. Okamoto I, Kawano Y, Matsumoto M et al (1999) Regulated CD44 cleavage under the control of protein kinase C, calcium influx, and the Rho family of small G proteins. J Biol Chem 274:25525–25534
65. Leavesley DI, Ferguson GD, Wayner EA et al (1992) Requirement of the integrin beta 3 subunit for carcinoma cell spreading or migration on vitronectin and fibrinogen. J Cell Biol 117:1101–1107
66. Platten M, Wick W, Wild-Bode C et al (2000) Transforming growth factors beta(1) (TGF-beta(1)) and TGF-beta(2) promote glioma cell migration via up-regulation of alpha(V)beta(3) integrin expression. Biochem Biophys Res Commun 268:607–611
67. Adachi Y, Lakka SS, Chandrasekar N et al (2001) Down-regulation of integrin alpha(v)beta(3) expression and integrin-mediated signaling in glioma cells by adenovirus-mediated transfer of antisense urokinase-type plasminogen activator receptor (uPAR) and sense p16 genes. J Biol Chem 276:47171–47177
68. Natarajan M, Stewart JE, Golemis EA et al (2006) HEF1 is a necessary and specific downstream effector of FAK that promotes the migration of glioblastoma cells. Oncogene 25:1721–1732
69. Liotta LA, Tryggvason K, Garbisa S et al (1980) Metastatic potential correlates with enzymatic degradation of basement membrane collagen. Nature 284:67–68
70. Wild-Bode C, Weller M, Wick W (2001) Molecular determinants of glioma cell migration and invasion. J Neurosurg 94:978–984
71. Li L, Gondi CS, Dinh DH et al (2007) Transfection with anti-p65 intrabody suppresses invasion and angiogenesis in glioma cells by blocking nuclear factor-kappaB transcriptional activity. Clin Cancer Res 13:2178–2190
72. Song H, Li Y, Lee J et al (2009) Low-density lipoprotein receptor-related protein 1 promotes cancer cell migration and invasion by inducing the expression of matrix metalloproteinases 2 and 9. Cancer Res 69:879–886
73. Wang H, Shen W, Huang H et al (2003) Insulin-like growth factor binding protein 2 enhances glioblastoma invasion by activating invasion-enhancing genes. Cancer Res 63:4315–4321
74. Baker AH, George SJ, Zaltsman AB et al (1999) Inhibition of invasion and induction of apoptotic cell death of cancer cell lines by overexpression of TIMP-3. Br J Cancer 79:1347–1355
75. Tonn JC, Kerkau S, Hanke A et al (1999) Effect of synthetic matrix-metalloproteinase inhibitors on invasive capacity and proliferation of human malignant gliomas in vitro. Int J Cancer 80:764–772
76. Tonn JC, Goldbrunner R (2003) Mechanisms of glioma cell invasion. Acta Neurochir Suppl 88:163–167
77. Beadle C, Assanah MC, Monzo P et al (2008) The role of myosin II in glioma invasion of the brain. Mol Biol Cell 19:3357–3368
78. Salhia B, Rutten F, Nakada M et al (2005) Inhibition of Rho-kinase affects astrocytoma morphology, motility, and invasion through activation of Rac1. Cancer Res 65:8792–8800
79. Bornhauser BC, Lindholm D (2005) MSAP enhances migration of C6 glioma cells through phosphorylation of the myosin regulatory light chain. Cell Mol Life Sci 62:1260–1266
80. Brat DJ, Mapstone TB (2003) Malignant glioma physiology: cellular response to hypoxia and its role in tumor progression. Ann Intern Med 138:659–668
81. Zagzag D, Zhong H, Scalzitti JM et al (2000) Expression of hypoxia-inducible factor 1alpha in brain tumors: association with angiogenesis, invasion, and progression. Cancer 88:2606–2618
82. Brat DJ, Castellano-Sanchez AA, Hunter SB et al (2004) Pseudopalisades in glioblastoma are hypoxic, express extracellular matrix proteases, and are formed by an actively migrating cell population. Cancer Res 64:920–927
83. Elstner A, Holtkamp N, von Deimling A (2007) Involvement of Hif-1 in desferrioxamine-induced invasion of glioblastoma cells. Clin Exp Metastasis 24:57–66
84. Martens T, Schmidt NO, Eckerich C et al (2006) A novel one-armed anti-c-Met antibody inhibits glioblastoma growth in vivo. Clin Cancer Res 12:6144–6152
85. Eckerich C, Zapf S, Fillbrandt R et al (2007) Hypoxia can induce c-Met expression in glioma cells and enhance SF/HGF-induced cell migration. Int J Cancer 121:276–283
86. Sathornsumetee S, Reardon DA, Desjardins A et al (2007) Molecularly targeted therapy for malignant glioma. Cancer 110:13–24
87. Vredenburgh JJ, Desjardins A, Herndon JE 2nd et al (2007) Phase II trial of bevacizumab and irinotecan in recurrent malignant glioma. Clin Cancer Res 13:1253–1259
88. Norden AD, Young GS, Setayesh K et al (2008) Bevacizumab for recurrent malignant gliomas: efficacy, toxicity, and patterns of recurrence. Neurology 70:779–787
89. Lamszus K, Kunkel P, Westphal M (2003) Invasion as limitation to anti-angiogenic glioma therapy. Acta Neurochir Suppl 88:169–177
90. Sathornsumetee S, Cao Y, Marcello JE et al (2008) Tumor angiogenic and hypoxic profiles predict radiographic response and survival in malignant astrocytoma patients treated with bevacizumab and irinotecan. J Clin Oncol 26:271–278
91. Bergers G, Hanahan D (2008) Modes of resistance to anti-angiogenic therapy. Nat Rev Cancer 8:592–603
92. MacDonald TJ, Taga T, Shimada H et al (2001) Preferential susceptibility of brain tumors to the antiangiogenic effects of an alpha(v) integrin antagonist. Neurosurgery 48:151–157
93. Fu Y, Ponce ML, Thill M, Yuan P et al (2007) Angiogenesis inhibition and choroidal neovascularization suppression by sustained delivery of an integrin antagonist, EMD478761. Invest Ophthalmol Vis Sci 48:5184–5190
94. Taga T, Suzuki A, Gonzalez-Gomez I et al (2002) alpha v-Integrin antagonist EMD 121974 induces apoptosis in brain tumor cells growing on vitronectin and tenascin. Int J Cancer 98:690–697
95. Eskens FA, Dumez H, Hoekstra R et al (2003) Phase I and pharmacokinetic study of continuous twice weekly intravenous administration of cilengitide (EMD 121974), a novel inhibitor of the integrins alphavbeta3 and alphavbeta5 in patients with advanced solid tumours. Eur J Cancer 39:917–926
96. Reardon DA, Fink KL, Mikkelsen T et al (2008) Randomized phase II study of cilengitide, an integrin-targeting arginine-glycine-aspartic acid peptide, in recurrent glioblastoma multiforme. J Clin Oncol 26:5610–5617
97. Reardon DA, Nabors LB, Stupp R et al (2008) Cilengitide: an integrin-targeting arginine–glycine–aspartic acid peptide with promising activity for glioblastoma multiforme. Exp Opin Invest Drugs 17:1225–1235
98. Levin VA, Phuphanich S, Yung WK et al (2006) Randomized, double-blind, placebo-controlled trial of marimastat in glioblastoma multiforme patients following surgery and irradiation. J Neurooncol 78:295–302
99. Groves MD, Puduvalli VK, Hess KR et al (2002) Phase II trial of temozolomide plus the matrix metalloproteinase inhibitor, marimastat, in recurrent and progressive glioblastoma multiforme. J Clin Oncol 20:1383–1388
100. D'Amato RJ, Loughnan MS, Flynn E et al (1994) Thalidomide is an inhibitor of angiogenesis. Proc Natl Acad Sci USA 91:4082–4085
101. Hansen JM, Harris C (2004) A novel hypothesis for thalidomide-induced limb teratogenesis: redox misregulation of the NF-kappaB pathway. Antioxid Redox Signal 6:1–14

102. Fine HA, Figg WD, Jaeckle K et al (2000) Phase II trial of the antiangiogenic agent thalidomide in patients with recurrent high-grade gliomas. J Clin Oncol 18:708–715
103. Adnane L, Trail PA, Taylor I, Wilhelm SM (2006) Sorafenib (BAY 43-9006, Nexavar), a dual-action inhibitor that targets RAF/MEK/ERK pathway in tumor cells and tyrosine kinases VEGFR/PDGFR in tumor vasculature. Methods Enzymol 407:597–612
104. Siegelin MD, Raskett CM, Gilbert CA, Ross AH, Altieri DC (2010) Sorafenib exerts anti-glioma activity in vitro and in vivo. Neurosci Lett 478:165–170
105. Kilic T, Alberta JA, Zdunek PR et al (2000) Intracranial inhibition of platelet-derived growth factor-mediated glioblastoma cell growth by an orally active kinase inhibitor of the 2-phenylaminopyrimidine class. Cancer Res 60:5143–5150
106. Ranza E, Mazzini G, Facoetti A, Nano R (2010) In vitro effects of the tyrosine kinase inhibitor imatinib on glioblastoma cell proliferation. J Neurooncol 96:349–357
107. Wen PY, Yung WK, Lamborn KR et al (2006) Phase I/II study of imatinib mesylate for recurrent malignant gliomas: North American Brain Tumor Consortium Study 99-08. Clin Cancer Res 12:4899–4907
108. Zagzag D, Shiff B, Jallo GI et al (2002) Tenascin-C promotes microvascular cell migration and phosphorylation of focal adhesion kinase. Cancer Res 62:2660–2668
109. Zagzag D, Friedlander DR, Dosik J et al (1996) Tenascin-C expression by angiogenic vessels in human astrocytomas and by human brain endothelial cells in vitro. Cancer Res 56:182–189
110. Bigner DD, Brown M, Coleman RE et al (1995) Phase I studies of treatment of malignant gliomas and neoplastic meningitis with 131I-radiolabeled monoclonal antibodies anti-tenascin 81C6 and anti-chondroitin proteoglycan sulfate Me1-14 F (ab′)2—a preliminary report. J Neurooncol 24:109–122
111. Reardon DA, Akabani G, Coleman RE et al (2002) Phase II trial of murine (131)I-labeled antitenascin monoclonal antibody 81C6 administered into surgically created resection cavities of patients with newly diagnosed malignant gliomas. J Clin Oncol 20:1389–1397

ARTICLE
Journal of Cellular Biochemistry 112:318-329 (2011)

Journal of Cellular Biochemistry

Extracellular Matrix Modulates Insulin Production During Differentiation of AR42J Cells: Functional Role of Pax6 Transcription Factor

Kohei Hamamoto,[1] Satoko Yamada,[1] Akemi Hara,[1] Tsutomu Kodera,[1,2] Masaharu Seno,[3] and Itaru Kojima[1*]

[1]*Institute for Molecular and Cellular Regulation, Gunma University, Maebashi, Japan*
[2]*Third Department of Internal Medicine, National Defence Medical College, Tokorozawa, Japan*
[3]*Graduate School of Natural Science, Okayama University, Okayama, Japan*

ABSTRACT

Extracellular matrix (ECM) modulates differentiation of pancreatic β-cells during development. However, the mechanism by which ECM proteins modulate differentiation is not totally clear. We investigated the effect of ECM proteins on differentiation β-cells in vitro. We investigated the effect of basement membrane ECM on differentiation of AR42J cells and rat ductal cells. First, we examined the effect of reconstituted basement membrane, Matrigel on differentiation of AR42J cells induced by activin and betacellulin. Matrigel augmented insulin production and increased the expression of GLUT2, SUR1, and glucokinase. Among various transcription factors investigated, Matrigel markedly upregulated the expression of Pax6. When Pax6 was overexpressed in cells treated with activin and betacellulin, the expression of insulin was upregulated. Conversely, knockdown of Pax6 significantly reduced the insulin expression in cells cultured on Matrigel. The effects of Matrigel on insulin-production and induction of Pax6 were reproduced partially by laminin-1, a major component of Matrigel, and inhibited by anti-integrin-β1 antibody. Matrigel also enhanced the activation of p38 mitogen-activated kinase induced by activin and betacellulin, which was inhibited by anti-β1 antibody. Finally, the effect of Matrigel on differentiation was reproduced in rat cultured ductal cells, and Matrigel also increased the expression of Pax6. These results indicate that basement membrane ECM augments differentiation of pancreatic progenitor cells to insulin-secreting cells by upregulating the expression of Pax6. J. Cell. Biochem. 112: 318–329, 2011. © 2010 Wiley-Liss, Inc.

KEY WORDS: DIFFERENTIATION; β-CELL; MATRIX; PAX6; ACTIVIN A; BETACELLULIN

Differentiation of pancreatic β-cell is strictly controlled by an integrated network of transcription factors. Homeobox transcription factors are important in regulating differentiation [Jonsson et al., 1994; Harrison et al., 1995; Offield et al., 1996; Ahlgren et al., 1997; Naya et al., 1997; Sosa-Pineda et al., 1997; Sussel et al., 1998; Li et al., 1999; Sander et al., 2000; Olbrot et al., 2002; Artner et al., 2007]. Among them, importance of the paired homeobox family is also demonstrated. Pax4-deficient mice lack differentiated β-and δ-cells, and fail to develop mature islets [Sosa-Pineda et al., 1997]. Severe reduction of all endocrine cell types and disruption of the islet architecture are observed in mice lacking Pax6 [Sander et al., 1997; St-Onge et al., 1997]. These transcription factors do not only regulate development but also act to maintain mature β-cell functions [Murtaugh, 2006]. Determination of the factors and molecular signals that regulate these transcription factors is essential not only for understanding the mechanism of pancreatic development but also for establishing the cell based therapy for diabetes.

The importance of extracellular matrix (ECM) in regulating adhesion, migration, proliferation, differentiation and maintenance of mature cell function is well demonstrated. In the pancreas, roles of the basement membrane and its components for islet development and β-cell functions are extensively investigated. For instance, in embryo, attachment to the basement membrane of fetal aorta promotes induction of pancreatic progenitor cells from undifferentiated endoderm [Lammert et al., 2001; Yoshitomi and Zaret, 2004]. Recent study using knockout mice with islet specific ablation of vascular endothelial cells shows severe reduction of β-cells, due to the loss of cell attachment to the basement membrane [Nikolova et al., 2006]. Also, laminin-1, one of the major components of the

*Correspondence to: Itaru Kojima, MD, Institute for Molecular & Cellular Regulation, Gunma University, 3-39-15 Showa-machi, Maebashi 371-8512, Japan. E-mail: ikojima@showa.gunma-u.ac.jp
Received 14 June 2010; Accepted 13 October 2010 • DOI 10.1002/jcb.22930 • © 2010 Wiley-Liss, Inc.
Published online 10 November 2010 in Wiley Online Library (wileyonlinelibrary.com).

basement membrane in fetal pancreas, induces differentiation of early pancreatic cells into insulin-positive cells in mice, whereas collagen type IV which is also an ECM component of the fetal pancreas has been shown to inhibit pancreatic development [Jiang et al., 1999].

In addition to the role of ECM, the importance of integrins are suggested. Integrins are heterodimeric glycoproteins composed of 18 α-subunits noncovalently linked to 8 β-subunits and provide a dynamic interaction of environmental cues and intracellular events by binding to their corresponding ECM [Hynes, 2002]. Of various integrins, the β1 integrin is important for islet development [Jiang et al., 2002; Wang et al., 2005; Yashpal et al., 2008]. Indeed, β1 integrin is broadly expressed in pancreatic epithelium, and in mice lacking β1 integrin, islet structure is disrupted [Kren et al., 2007].

In general, signals from ECM or integrin receptors control cell differentiation by altering the expression of transcriptional factors [Riquelme et al., 2001; Suzuki et al., 2003]. Therefore, the role of cell–matrix interaction on the regulatory network of transcription factors that control pancreatic development is postulated. However, information as to this link is limited. Yoshitomi and Zaret [2004] showed that attachment to aortic endothelial cells induces the expression of Ptf1a in dorsal pancreatic endoderm. They also showed that contact with the basement membrane was required for maintenance of Pdx1 expression in dorsal pancreas. This study demonstrates that signals from ECM modulate pancreatic development by induction of transcriptional factors, but the precise role of ECM or their receptor integrins in the regulation of transcriptional factors is unclear.

In the present study, we investigated the effect of the cell–matrix interaction on differentiation of pancreatic β-cells, in particular, its effect on regulation of transcription factors. By using AR42J cells, a model cell system to study the processes of endocrine differentiation [Mashima et al., 1996], we found that reconstituted basement membrane Matrigel promotes endocrine differentiation, at least in part, by inducing Pax6. In addition, we also found that some of these effects are dependent on laminin-1 and transmitted by the β1 integrin signaling.

MATERIALS AND METHODS

MATERIALS

Recombinant human activin A was provided by Dr. Y. Eto (Central Research Laboratory, Ajinomoto, Kawasaki, Japan). Recombinant human betacellulin (BTC) was prepared as described previously [Seno et al., 1996].

CELL CULTURE

AR42J cells were cultured in Dulbecco's modified Eagle's medium (DMEM) containing 10% fetal bovine serum (FBS) [Mashima et al., 1996]. Cells were incubated with a combination of activin A and BTC to induce differentiation. To evaluate the effect of anti-β1 integrin blocking antibody, cells were resuspended in DMEM containing 10% FBS and preincubated for 15 min with 10 μg/ml anti-β1 blocking antibody (Ha 2/5, BD Biosciences Japan, Tokyo, Japan) or purified hamster IgM before plating.

Rat pancreatic ductal cells were cultured as described previously [Ogata et al., 2004]. More than 95% of the cells were positive for cytokeratin, and cells positive for immunoreactive insulin were not observed before differentiation.

COATING OF DISHES AND SLIDES

Petri dishes (100 mm in diameter) were coated with 25 $\mu g/cm^2$ growth factor-reduced Matrigel, 5 $\mu g/cm^2$ human fibronectin, 10 $\mu g/cm^2$ laminin, 10 $\mu g/cm^2$ collagen type-IV. All extracellular matrices were purchased from BD Biosciences Japan. For morphological and immunohistochemical analyses, glass coverslips were coated with the same concentrations of matrices. In each experiment, 5% bovine serum albumin (BSA) (Sigma–Aldrich Japan, Tokyo, Japan) in phosphate-buffered saline (PBS) was used as a control.

PREPARATION OF RECOMBINANT ADENOVIRUSES

Recombinant adenovirus expressing Pax6 was prepared using a Virapower™ Adenoviral Gateway Expression kit (Invitrogen Japan, Tokyo, Japan). In brief, coding region of mouse Pax6 was digested from plasmid vector encoding mouse Pax6 (pBAT14-mPax6, kindly provided by Dr. Michel German, UCSF, San Francisco, CA) and cloned into an entry vector pENTR3C. To create expression clones and produce recombinant adenovirus, transfer of the mouse Pax6 cassette into the destination vector containing human CMV promoter (pAd/CMV/V5-DEST, Invitrogen Japan) by LR recombination reaction, linearization of plasmid with Pac I and transfection into Adenovirus expressing siRNA for rat Pax6 was constructed using the following oligonucleotide: 5′-CACCGGGTCTGTACCAACGACAATACGAATATTGTCGTTGGTACAGACCC-3′. This oligonucleotide was inserted in the pENTR/U6 entry vector (Invitrogen Japan). Subsequently, U6/shRNAs cassettes were transferred into the destination vector (pAd/BLOCK-iT-DEST, Invitrogen Japan) by LR recombination. Following linearization of plasmid, transfection into 293 cells was performed.

MORPHOLOGICAL ANALYSIS AND IMMUNOHISTOCHEMISTRY

AR42J cells cultured on BSA or matrix-coated glasses were fixed, treated with 0.1% Triton X-100, and then blocked with Blocking Ace solution (Morinaga, Tokyo, Japan). Primary antibodies used were mouse anti-swain insulin (1:100, Spring Bioscience, Freemont, CA), rabbit anti-rat Pax6 (Covance, Berkeley, CA), and rabbit anti-human glucagon (1:100, Dako, Glostrup, Denmark, CA). Secondary antibodies were as follows: biotinylated anti-mouse IgG and biotinylated anti-rabbit IgG (1:400, Vector Laboratories, Brulingam, CA). The fluorescent signals were detected by avidin-conjugated AlexaFluor488 (Molecular Probes, Inc., Eugene, OR). For double-staining, Alexa Fluor568-conjugated anti-mouse IgG and Alexa568-conjugated anti-rabbit IgG (1:600) were used as secondary antibodies.

RNA ISOLATION AND RT-PCR

Total RNA was isolated using TRIZOL reagent (Invitrogen Japan). Total RNA samples were pretreated with DNase I (Nippon gene, Tokyo, Japan) to remove contamination of genomic DNA. First-strand cDNA was synthesized by the SuperScript™III first strand

synthesis system (Invitrogen Japan). Oligonucleotide-primers and PCR-reaction conditions were as previously mentioned [Zhang et al., 2001], except for rat insulin 1 (5′-TACAATCATAGACCAT-CAGCAAGC-3′ and 5′-CAGTTGGTAGAGGGAGCAGAT-3′ initial denaturation at 95°C for 5 min followed by 35 cycles of 94°C for 30 s, 60°C for 30 s, 68°C for 30 s), rat insulin 2 (5′-AGCCCTAAGT-GAACCAGCTACA-3′ and 5′-TGCCAAGGTCTGAAGGTCAC-3′, initial denaturation at 95°C for 5 min followed by 36 cycles of 94°C for 30 s, 60°C for 30 s, 68°C for 30 s), neurogenin-3 (5′-TTCGCA-CAGTTCCTTGCTGC-3′ and 5′-CGCAACACTGGATTAGGTCACTC-3′ initial denaturation at 95°C for 5 min followed by 32 cycles of 94°C for 30 s, 60°C for 30 s, 72°C for 30 s), and MafA (5′-GATGAAGTTC-GAGGTGAAGA-3′ and 5′-GCTCATCCAGTACAGATCCT-3′ initial denaturation at 95°C for 5 min followed by 35 cycles of 94°C for 30 s, 60°C for 30 s, 72°C for 30 s).

REAL-TIME PCR ANALYSIS

One microliter of the first-strand cDNA obtained as described above was used in a 20-μl reaction mixture including 1× SYBR greenER qPCR SuperMix (Invitrogen Japan) and 150 nM primer for rat insulin 2 primer, 200 nM primer for rat Pax6 (5′-CACCGCCCTCACCAACAC-3′ and 5′ GCAGG AGTACGAGGAGGTCTGA-3′), and 200 nM for rat GAPDH (5′-CATGACCACAGTCCATGCCATC-3′; anti-sense, 5′-CACCCTGTTGCTGTAGCCATATTC-3′). The initial cycling conditions involved a hold at 95°C for 10 min, followed by 40 cycles of 94°C for 15 s, then 60°C for 60 s. The signal fluorescence magnitude was detected with an ABI PRISM 7500 Sequence Detector System. Data were normalized to GAPDH signals and presented as mean ± SE.

IMMUNOBLOTTING

Cells were suspended in Laemmli buffer and heated to 100°C for 10 min. After centrifugation, the supernatant was collected, and protein concentration was measured by a BCA protein assay kit (Pierce, Rockford, IL). Cell lysate proteins were separated by 10% sodium dodecyl sulfate polyacrylamide gel electrophoresis, and transferred to polyvinylidene fluoride membrane (Millipore Japan, Tokyo, Japan). The membranes were washed in Tris buffered-saline containing 0.1% Tween-20 and blocked with 5% nonfat dry milk overnight at 4°C. Immunoblotting was performed with the phospho-p42/44 mitogen-activated protein kinase (MAPK), phopho-p38 MAPK, p42/44 MAPK, and p38 detected by chemiluminescence reagents (LumiGLO, Cell Signaling Technology Japan), and the chemiluminescence signals were detected by an image analyzer system (LAS-3000, Fujifilm, Tokyo, Japan).

ELISA FOR INSULIN

Whole cell extracts were obtained by treatment for 24 h on ice in acid–ethanol. The insulin content was determined using Insulin ELISA kit/Rat Ultra Sensitive using rodent insulin standard (Morinaga Biochemicals, Yokohama, Japan), and rat insulinoma INS-1 was used as a positive control. Insulin concentration was normalized with total cellular protein, measured using the BCA protein assay kit (Pierce).

STATISTICAL ANALYSIS

Values are expressed as mean ± SE. The statistical significance was determined using a two-tailed unpaired Student's *t*-test, and differences were considered to be statistically significant when $P < 0.05$.

RESULTS

EFFECT OF RECONSTITUTED BASEMENT MEMBRANE ON DIFFERENTIATION

Previous studies suggested the importance of the basement for pancreatic development [Jiang et al., 1999; Bonner-Weir et al., 2000; Lammert et al., 2001; Yoshitomi and Zaret, 2004; Nikolova et al., 2006]. We first investigated the role of reconstituted basement membrane, Matrigel, on cell differentiation in AR42J cells. We first characterized cell adhesion and morphology in cells cultured on Matrigel-coated or BSA-coated dish (control dish). As shown in Figure 1A-a, naive AR42J cells were round-shaped on the control dish, and time required for majority of the cells to attach to the dish was approximately 12 h. When cells were cultured on Matrigel-coated dishes, cells adhered quite rapidly, and majority of the cells adhered within 30 min (Fig. 1B). When attached, they rapidly flattened and presented spindle-shaped appearances (Fig. 1A-b) which were comparable to those observed in activin-treated cells as previously reported [Ohnishi et al., 1995]. These relatively flattened and spread-shaped appearances were also observed in cells cultured on Matrigel in the presence of BTC and activin (differentiated cells). In differentiated cells cultured on Matrigel, cell size was increased and relatively longer, and multiple processes compared to those cultured on control dish were observed (Fig. 1A-c,A-d). We next measured the expression of mRNA for pancreatic hormones. As previously described [Ohnishi et al., 1995], we confirmed the absence of pancreatic hormones in naive AR42J cell, whereas induction of insulin-2 and pancreatic polypeptide (PP) in differentiated cells (Fig. 1C). Although these expression patterns were unchanged even in cells cultured on Matrigel, we found a remarkable increase in mRNA for insulin-2 in cells cultured on Matrigel. Quantitative RT-PCR analysis demonstrated an approximately sevenfold higher expression of insulin-2 in cells cultured on Matrigel ($P < 0.05$, Fig. 1D). We next performed immunohistochemistry to examine distribution of insulin signals. As shown in Figure 1E, insulin signals were detected in the tips of cell processes in the majority the cells cultured on control dishes. In contrast, cells cultured on Matrigel showed a broadly cytoplasmic distribution of insulin signals. In addition, the signal intensities of insulin in cells cultured on Matrigel were stronger. On the other hand, insulin signals were not detected in naive cells. Consistent with the results obtained by immunohistochemistry, we found approximately twofold increase in insulin content in differentiated cells cultured on Matrigel ($P < 0.05$, Fig. 1F). We further measured the expression of β-cell-associated molecules including GLUT2, glucokinase, SUR1 and Kir6.2, and neuroendocrine markers including PGP9.5, synaptophysin and tyrosine hydroxylase. As reported previously, the expression of GLUT2, SUR1, and glucokinase (Fig. 1G) was induced by the treatment with activin and BTC. In addition, induction of the expression of mRNA for Kir6.2 and tyrosine

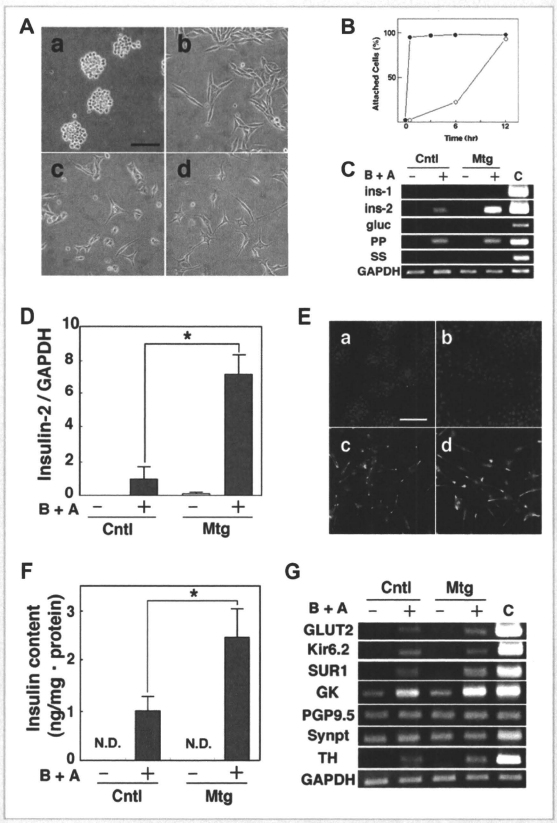

Fig. 1. Effect of reconstituted basement membrane on differentiation of AR42J cells. A: Cell Morphology. AR42J cells (1×10^5 cells/35 mm-dish) were plated on BSA (control matrix) (a,c)-coated and Matrigel (b,d)-coated dishes and incubated for 48 h with (c,d) or without (a,b) 1 nM BTC and 2 nM activin A. Phase contrast micrographs are presented. Bar = 100 μm. B: Time course of effect of matrigel on cell adhesion. Cell were plated on BSA- (○) and matrigel-coated (●) dishes for various periods and the number of attached cells was counted. Values are the mean of three experiments. C: Expression of mRNA for pancreatic hormones. Cells (6×10^5 cells/100 mm-dish) were incubated for 48 h with (+) or without (−) 1 nM BTC and 2 nM activin A (B + A) in control and Matrigel-(Mtg)-coated dishes. The expression of mRNA for insulin-1 (ins-1), insulin-2 (ins 2), glucagon (gluc), pancreatic polypeptide (PP), and somatostatin (SS) was analyzed by RT-PCR. GAPDH serves as a control. mRNA obtained from rat pancreas was used as a positive control (c). Cntl: control, Mtg: Matrigel. D: Quantification of mRNA for insulin-2. Cells were incubated as described in (A), and the expression of mRNA for insulin was quantified by real-time PCR. Results are the mean ± SE for three experiments. *$P < 0.05$. Cntl: control, Mtg: Matrigel. E: Insulin-staining of differentiated cells. Cells were cultured on control dish (a,c) or Matrigel-coated (b,d) dishes and incubated for 48 h with (c,d) or without (a,b) 2 nM activin A and 1 nM BTC. Staining of insulin by immunofluorescence was obtained. A broad cytoplasmic staining pattern of insulin was observed in differentiated cells cultured on Matrigel (d). Nuclei were stained with 4′, 6-diamidino-2-phenylindole (DAPI). Bar = 100 μm. Cntl: control, Mtg: Matrigel. F: Changes in the insulin content. Cells were treated as described above, and changes in the insulin content and total cellular protein were measured. The normalized values are the mean ± SE for three independent experiments. ND, not detectable. *$P < 0.05$. Cntl: control, Mtg: Matrigel. G: Changes in the expression of mRNA for islet-associated Molecules. Cells were cultured on control (Cntl) or Matrigel-coated (Mtg) dishes and incubated for 48 h with (+) or without (−) activin A and BTC. mRNA for GLUT2, Kir6.2, SUR1, and glukokinase (GK) were measured by RT-PCR. C: mRNA obtained from INS-1 cells.

hydroxylase was observed. These expression patterns were also observed in cells cultured on Matrigel, but the expression of mRNA for SUR1, glucokinase, and tyrosine hydroxyrase was increased. The expression of mRNA for PGP9.5 and synaptophysin was detected in cells cultured on control dishes and Matrigel, and there were no significant changes during the differentiation. These results suggest that Matrigel promotes differentiation in AR42J cells.

CHANGES IN THE EXPRESSION OF ISLET CELL ASSOCIATED TRANSCRIPTION FACTORS

To determine whether the effect of Matrigel on β-cell differentiation involves changes in the expression of transcriptional factors, we investigated mRNA for islet-associated transcription factors by RT-PCR. As shown in Figure 2A, we found that the expression of Pdx-1, Nkx2.1, Beta2, cdx2/3, cdx4, and lmx1.2 were detected in cells cultured on control dishes and Matrigel, and there were no significant changes during differentiation. The mRNA for Nkx6.1, Isl-1, HB9 and MafA was undetectable before and after differentiation in cells cultured on control dishes and Matrigel. The mRNA for lmx2, lmx1.1, Pax4, Hox1.11, and neurogenin3 was increased during differentiation in cells cultured on control dishes and Matrigel, and there were no significant differences. The mRNA for Pax6 was up-regulated during differentiation in cells cultured on control dishes and Matrigel. However, the expression level was higher in cells cultured on Matrigel. By quantitative RT-PCR, we found an approximately fivefold higher expression of Pax6 in cells cultured on Matrigel (Fig. 2B).

FUNCTIONAL ROLE OF PAX6

The above results indicate that Matrigel induces the expression of Pax6 during differentiation. Previous reports showed that Pax6 promoted transcription of insulin [Sander et al., 1997]. We speculated that Pax6 may be involved in the increase in the insulin expression. To assess the significance of Pax6, we first transfected an adenovirus vector encoding Pax6 into cells cultured on control dishes. To effectively identify transfected cells, we measured immunofluorescence using anti-Pax6 antibody. Some Pax6-transfected cells induced morphological changes, which included relatively longer neurite-like processes (Fig. 3A). In addition, these cells presented relatively intense signals of insulin with broadly cytoplasmic localization. Consistent with results obtained by immunohistochemistry, quantitative RT-PCR analysis demonstrated an approximately fivefold increase in the expression of mRNA for insulin-2 in Pax6-transfected cells ($P < 0.05$, Fig. 3B). However, the expression levels of insulin-2 in Pax6-transfected cells were lower than that of untransfected cells cultured on Matrigel ($P < 0.05$). Effect of combination of Matrigel and Ad-Pax6 was nearly identical to that of Matrigel alone. Furthermore, Pax6-transfected cells expressed glucagon and somatostatin by RT-PCR analysis (data not shown). To further investigate the functional role of Pax6, we also

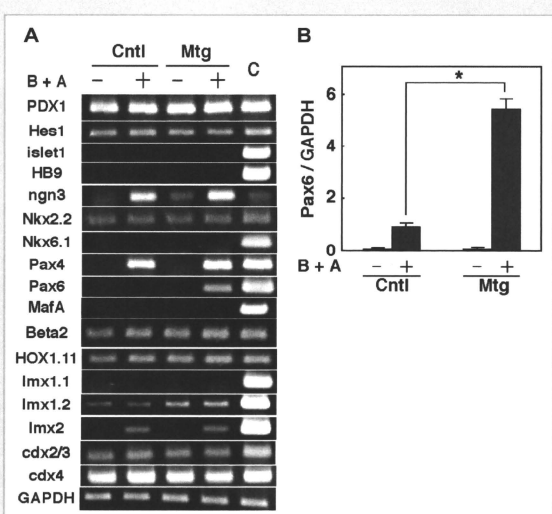

Fig. 2. Effect of matrigel on the expression of mRNA for islet-related transcription factors. A: Changes in mRNA for islet-related transcription factors. Cells were cultured on BSA- (Cntl) or matrigel-coated (Mtg) dishes and incubated for 48 h with (+) or without (−) 1 nM betacellulin and 2 nM activin A (B + A). mRNA from INS-1 cells was used as a positive control (c). B: Quantification of the expression of mRNA for Pax6. Cells were incubated as indicated in (A), and real-time RCR analysis of mRNA for Pax6 was performed. Results are the mean ± SE for four experiments. *$P < 0.05$.